ISBN: 978-3-95450-238-7 ISSN: 2226-0358 doi:10.18429/JACoW-ICALEPCS2023-TUPDP117

CLASSIFICATION AND PREDICTION OF SUPERCONDUCTING MAGNET QUENCHES

J. Einstein-Curtis *, J. P, Edelen, M. Kilpatrick, R. O'Rourke, RadiaSoft LLC, Boulder, Colorado
K. A. Drees, J. S. Laster, M. Valette, BNL, Upton, New York

Abstract

Robust and reliable quench detection for superconducting magnets is increasingly important as facilities push the boundaries of intensity and operational runtime. RadiaSoft has been working with Brookhaven National Lab on quench detection and prediction for superconducting magnets installed in the RHIC storage rings. This project has analyzed several years of power supply and beam position monitor data to train automated classification tools and automated quench precursor determination based on input sequences. Classification was performed using supervised multilayer perceptron and boosted decision tree architectures, while models of the expected operation of the ring were developed using a variety of autoencoder architectures. We have continued efforts to maximize area under the receiver operating characteristic curve for the multiple classification problem of real quench, fake quench, and no-quench events. We have also begun work on long short-term memory (LSTM) and other recurrent architectures for quench prediction. Examinations of future work utilizing more robust architectures, such as variational autoencoders and Siamese models, as well as methods necessary for uncertainty quantification will be discussed.

INTRODUCTION

Quench protection systems have been in service since the advent of superconducting magnet technology [1, 2]. In spite of the long history of quench detection technology, there has been a continuous effort to improve quench protection through the 90's with the construction of the LHC [3, 4] and in the 2000's with the construction of large detector magnets such as CMS [5] and the MICE experiment [6]. For a single magnet, once a quench is detected the power supply is switched off and then the magnet energy dumped into a load resister through a cold diode. When concerned with multiple magnets either bridge circuits or isolation amplifiers are usually considered [7]. For the MICE experiment for example, the magnet is divided into subdivisions in order to reduce the impact of a quench in a single subdivision. At RHIC there are multiple magnets chained together which introduces additional complexity [8]. In addition to the hardware requirements for protecting the magnet from quench events, there have been a number of efforts to ensure robust timing and triggering systems for coordinating the different quench protection systems and to ensure there is not a dirty beam dump. At RHIC, specifically, a redundant fiber optic communications system has been developed and installed to ensure effective permitting [9].

In addition to refining quench protection systems, quench detection also remains an area of interest. Traditional quench detection relies on measurement of the magnet resistance through the voltage and current delivered by the power supply. More recently efforts to identify quenches in advance to take preventative action has led to some interesting developments. For example, computation of the parasitic capacitance has demonstrated early detection of quench events [10]. Additional efforts have focused on using acoustic sensors to detect quenches [11]. This method monitors the change in the magnet's acoustic transfer function induced by a local temperature rise or an epoxy crack. In fact, a recent machine learning effort to detect precursors to magnet quenches using similar acoustic data has been quite successful [12]. While these methods show significant promise, much work can be done to refine the machine learning methods and to integrate them with operational accelerators. Here we develop tools for the classification of quench events in the hopes of being able to detect quench precursors in power supply or BPM data. We begin with qn overview of our dataset and then provide details for our quench classification results.

QUENCH DATA AND INITIAL ANALYSIS

The data included in our studies are from two separate datasets provided by BNL: beam position monitor (BPM) and power supply (PS). The original data was received as text files for each device, inside a hierarchy of directories representing the run, fill number, event type, and ring. The BPM text files contain timestamped beam position, difference, and coherence data at 10 kHz for 100 milliseconds around the event. The PS text files contain timestamped reference current, current, voltage, and voltage error data at 720 Hz for the 3 seconds leading up to the event and 1 second after the event. Additionally, Excel files were provided by BNL that contain information about the events, including the names of the specific power supply device names that were involved in reporting a quench event.

Before development of our ML models, it was first necessary to determine the characteristics of the data to determine the necessity of any additional data pre-processing. This included detailed investigations of the data itself around quench events, including gaining an understanding of the proper data sampling periods, expected signal behavior, and if there are any sort of label generation methods readily available. We also performed metadata analyses of the devices involved in the quenches; histograms of these studies can be seen in Figures 1 and 2.

Examining individual waveforms, we determined that quench vs non-quench datasets can be identified with high

* joshec@radiasoft.net

ISBN: 978-3-95450-238-7 ISSN: 2226-0358 doi:10.18429/JACoW-ICALEPCS2023-TUPDP117

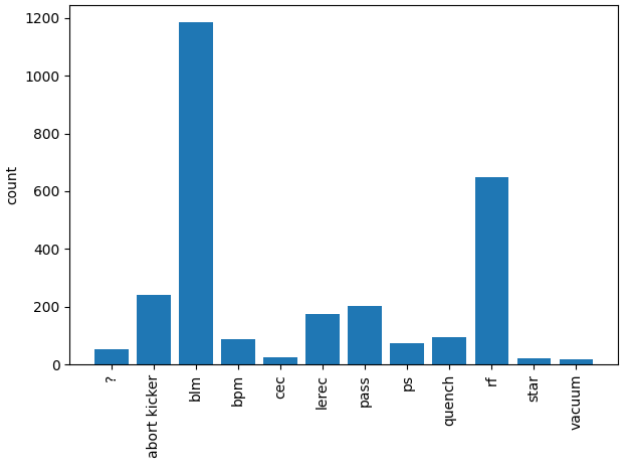

Figure 1: Histogram of reasons a quench occurred.

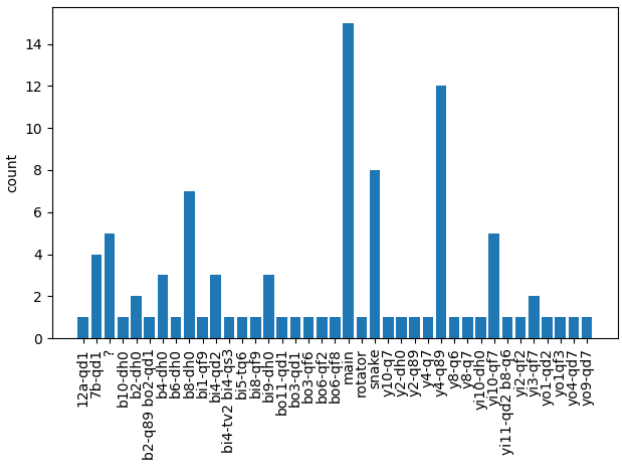

Figure 2: Histogram of the number of quenches that were caused by a specific device.

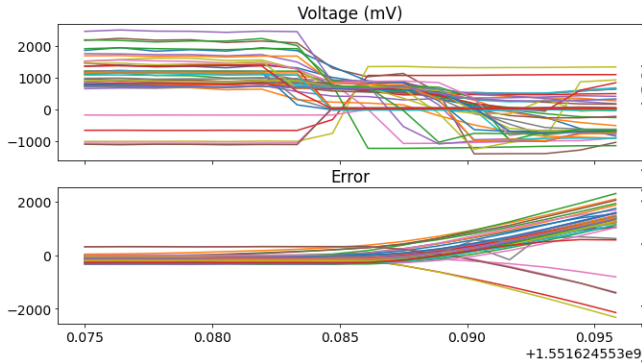

Figure 3: Voltage and error signals as measured by power supplies during a quench event. The data is triggered such that data before and after a trigger is logged.

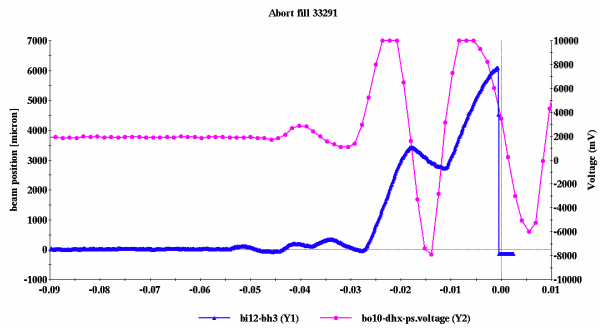

Figure 4: Beam position and voltage of a power supply during a quench event. Notice the beam position oscillating significantly before the power supply shuts off.

confidence by looking at standard deviations of the waveforms; this was used to generate a set of labels for use in ML applications. These labels provides us with the ability to verify the performance of our quench detection ML algorithms using a non-machine learning method, while also allowing for the use of supervised training methods. One of the more interesting considerations with these datasets is the inclusion of derived data; the reference current and error measurements are generally calculated based on other data, and are not purely recorded observables. This is important to keep in mind when looking at dependent variables and causation as ML models can be trained to *find* relationships that might not be physically possible. Examples of the waveforms collected during a quench event can be seen in Figures 3 and 4.

The text files and Excel files were parsed and converted into per-run Hierarchical Data Format (HDF5) files [13]. The HDF5 files store the datasets in a similar hierarchy to the directories they were received in (groups for run, fill number, event type, and ring), along with additional data from the Excel files stored as metadata attributes on their associated dataset. While generating the HDF5 file, the parser performs validation checks on each dataset and skips invalid data. This includes files that contained error messages and files that contain all zero data. Initial data collection and preprocessing found a large number of files that were messages reporting no data available or an error message output from automated data collection scripts being run at BNL, for example. Several iterations of data aggregation was performed to clan up a majority of these errors, with others handled by these validation checks. After parsing for valid data, we were left with 67264 BPM datasets and 32845 PS datasets. Of these PS datasets, 478 were from devices recorded as quench events and 32367 were due to non-quench events. All the datasets that were collected for both BPM and PS data were due to machine aborts; not every device in every dataset saw the abort events, outside of machine-wide events (e.g., facility-wide power disruption).

A Python class called `DataManager` was created as an interface to read the data from HDF5 files and return it in a format to be used as input for machine learning pipelines. `DataManager` returns a NumPy array with 3 dimensions representing the number of datasets, timestamps within the dataset, and data points at each timestamp, along with an associated metadata list. The `DataManager` interface allows for filtering by run, event type, and whether the device was listed as the Quenched PS for the event in the Excel

ISBN: 978-3-95450-238-7 ISSN: 2226-0358 doi:10.18429/JACoW-ICALEPCS2023-TUPDP117

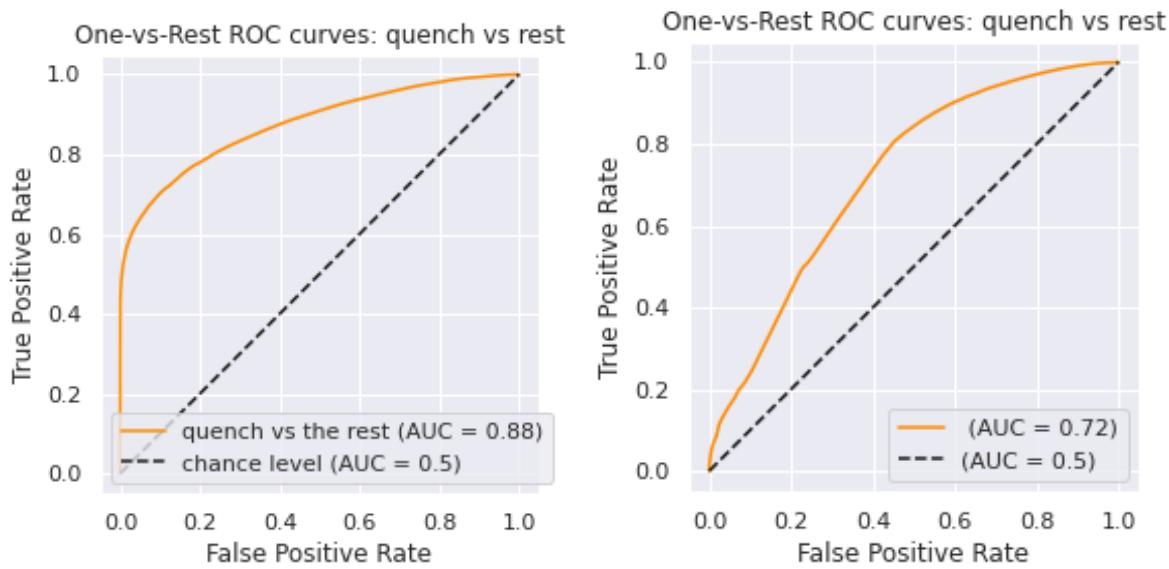

Figure 5: The quench-vs-rest ROC curves for PS (left) and BPM (right) using a BDT.

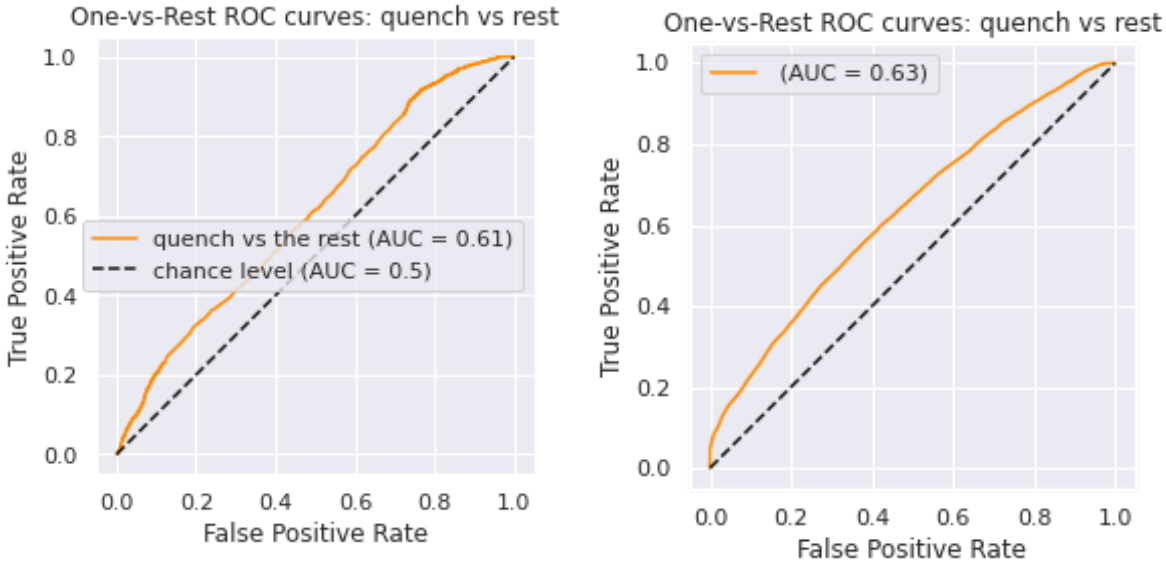

Figure 6: The quench vs rest ROC curves for BPM using a MLP classifier over a small data slice on the left. On the right, is quench vs rest ROC curves for PS data using a MLP classifier over the entire dataset.

file. `DataManager` also provides the labels for each dataset returned in the array.

This sort of Python module allows for better version control and consistent operation across multiple users and experiments without as many concerns over reproducibility.

QUENCH CLASSIFICATION

With the application of the `DataManager` to parse and organize our datasets into easily managed HDF5 files, we split datasets by label and used classification algorithms to reconstruct each dataset. We investigated two main methods for classification. The first method is a Boosted Decision Tree (BDT) [14] with regression for both single and multi-classification for BPM and PS datasets. The second is a custom developed Multi-Layer Perceptron (MLP) trained on a slice of the dataset near a quench event.

The BDT defines a set of nodes and leaves to split data with the goal of maximizing the information gained from the data or minimizing entropy, where there is a maximum for a 0.50/0.50 split and minimum for a 1/0 split. The tree is boosted using the ensemble weight of each misclassified event for further training. Our PS dataset has 5 distinguishable labels: `snake`, `main`, `rotator`, `?`, and `quench`, while the BPM dataset has 4 distinguishable labels: ps, blm, bpm, and quench. The BPM dataset has other labels, but they are indistinguishable from each other, so they are ignored within the classification.

Receiver operating characteristic (ROC) curves are used in classification problems as a visual representation of model

ISBN: 978-3-95450-238-7 ISSN: 2226-0358 doi:10.18429/JACoW-ICALEPCS2023-TUPDP117

performance, with their area under the curve (AUC) a key single metric derived from this. ROC curves for the PS and BPM data that is labeled as quench vs the rest of the dataset, also known as one-vs-rest, can be seen in Figure 5. The PS data performs well with a large ROC-AUC of 0.88, which means there are some distinguishable features within the data used as input to the model to classify quench events. The BPM data shows a slightly worse ROC-AUC of 0.72, but this shows that the model has a decent ability to correctly classify the given input data as quench events. Both of these models were trained over a full period, where the quench event can be clearly seen in input data.

An MLP classification model was also developed to perform a similar classification for both the BPM and power supply data, as the arrangement of fully-connected layers can often find different sorts of connections between data in training. The MLP classifier is constructed of fully-connected layers of sizes [500,200,50,number_of_labels], with the input data flattened. Figure 6 shows the quench-vs-rest ROC curve using indices [650:850] of the 1024-point input vector for classification. This shows possible precursors in the BPM data for quench prediction due to the better than 0.5 ROC-AUC. The data shown on the right of Figure 6 shows a better ROC-AUC, but is also trained over the entire dataset; a much higher ROC-AUC is expected given the characteristics of the data and the BDT results. It is possible that the MLP classifier issues with the PS data could be due to the need for different data pre-processing needs, but additional work still needs to be performed to clarify the reasons for this performance.

CONCLUSIONS

Our results on quench classification show that there are distinguishing features that can be used to train either a boosted decision tree or a neural network to label different types of quenches. This was accomplished using data collected from Brookhaven National Laboratory and a collaboration between RadiaSoft staff and BNL staff. Our methods utilized both BPM data and power supply data.

ACKNOWLEDGEMENTS

This material is based upon work supported by the U.S. Department of Energy, Office of Science, Office of High Energy Physics under Award Number DE-SC0021699.

REFERENCES

[1] P. F. Smith, "Protection of superconducting coils", *Rev. Sci. Instrum.*, vol. 34, no. 4, pp. 368–373, 1963. doi:10.1063/1.1718368

[2] K. E. Robins, W. B. Sampson, and M. G. Thomas, "Superconducting magnet quench protection for ISABELLE", *IEEE Trans. Nucl. Sci.*, vol. 24, no. 3, pp. 1318–1319, 1977. doi:10.1109/TNS.1977.4328930

[3] L. Coull, D. Hagedorn, V. Remondino, and F. Rodriguez-Mateos, "LHC magnet quench protection system", *IEEE Trans. Magn.*, vol. 30, no. 4, pp. 1742–1745, 1994. doi:10.1109/20.305593

[4] L. Salasoo, "Superconducting magnet quench protection analysis and design", *IEEE Trans. Magn.*, vol. 27, no. 2, pp. 1908–1911, 1991. doi:10.1109/20.133573

[5] P. Fazilleau *et al.*, "Analysis and design of the CMS magnet quench protection", *IEEE Trans. Appl. Supercond.*, vol. 16, no. 2, pp. 1753–1756, 2006. doi:10.1109/TASC.2006.873267

[6] X. L. Guo *et al.*, "Quench protection for the MICE cooling channel coupling magnet", *IEEE Trans. Appl. Supercond.*, vol. 19, no. 3, pp. 1360–1363, 2009. doi:10.1109/TASC.2009.2018054

[7] K. Mess, "Quench protection", in *CAS - CERN Accelerator School : Superconductivity in Particle Accelerators*. CERN, 1996, pp. 143–165. doi:10.5170/CERN-1996-003.143

[8] M. Anerella *et al.*, "The RHIC magnet system", *Nucl. Instrum. Methods Phys. Res. A*, vol. 499, no. 2, pp. 280–315, 2003. doi:10.1016/S0168-9002(02)01940-X

[9] C. Conkling, "RHIC beam permit and quench detection communications system", in *Proc. PAC'97*, vol. 2, 1997, pp. 2496–2498. doi:10.1109/PAC.1997.751252

[10] E. Ravaioli *et al.*, "A new quench detection method for HTS magnets: Stray-capacitance change monitoring", *Phys. Scr.*, vol. 95, no. 1, p. 015 002, 2019. doi:10.1088/1402-4896/ab4570

[11] A. Ninomiya, K. Sakaniwa, H. Kado, T. Ishigohka, and Y. Higo, "Quench detection of superconducting magnets using ultrasonic wave", *IEEE Trans. Magn.*, vol. 25, no. 2, pp. 1520–1523, 1989. doi:10.1109/20.92585

[12] D. Hoang *et al.*, "Intelliquench: An adaptive machine learning system for detection of superconducting magnet quenches", *IEEE Trans. Appl. Supercond.*, vol. 31, no. 5, pp. 1–5, 2021. doi:10.1109/TASC.2021.3058229

[13] Hierarchical Data Format, version 5, https://www.hdfgroup.org/HDF5/

[14] J. H. Friedman, "Greedy function approximation: A gradient boosting machine", *Ann. Stat.*, vol. 29, pp. 1189–1232, 2001.